Zinc Oxide Nanowire Field Effect Transistor Used as a pH Sensor

N. M. J. Ditshego
Electrical, Computer, and Telecommunications Engineering Department, CET, Botswana International University of Science and Technology, Private bag 16, Palapye, Botswana
Email: ditshegon@biust.ac.bw

***Abstract*—An ion sensitive field effect transistor can out-perform conventional ion-selective electrodes. Thus, a zinc oxide (ZnO) nanowire field effect transistor (NWFET) pH sensor was fabricated and measured. The sensor contained a channel with 1.7×10^{18} cm^{-3} donor concentration and 100 ZnO nanowires in parallel, each with the following dimensions: 10 µm×120 nm×20 nm. The active channel is passivated with an 18 nm Al_2O_3 layer. The device was measured under a controlled environment with and without pH solutions. The pH range was 3–9 with a sensitivity of 2.48 mV to 10.3 mV. The voltage sensitivity translates to a percentage value of 15%. The measurements obtained before and after the pH solution treatment demonstrate the possibility of re-use of the device by rinsing and brushing the sensing layer.**

***Index Terms*—Device sensitivity; ion sensitive field effect transistor; nanowire; pH sensor; zinc oxide (ZnO)**

I. Introduction

J. C. Dutta [1] asserts that ion sensitive field effect transistors (ISFETs) were first reported by Bergveld in 1970. In the past 19 years, research on these devices has increased as they tend to out-perform their counterparts (conventional ion-selective electrodes). The advantages [1] include a higher sensitivity, the use of 'lab-on-chip' systems, mass production at a small scale with a low cost, usability at a wide range of temperatures, multi-functionality, the ability to be converted into biosensors, and re-usability, as they are robust, durable, and can be cleaned with a toothbrush [1].

In the future, the fabricated device can be converted into a biosensor [2]. pH sensors are the first step toward biosensing because they provide a more coherent measurement than that of a protein sensor as they have more ionic charge [3]-[5]. The charge is distinguishable depending on the acidity or alkalinity of the solution. In addition, they do not require functionalization of the sensing window, which simplifies the fabrication process [6]. To the best of my knowledge, the studies began in 2013, and the first successful pH sensor was created on passivated ZnO NWFET using the spacer fabrication method.

Manuscript received July 17, 2021; revised October 21, 2021; accepted November 2, 2021.
Corresponding author: N. M. J. Ditshego (email: ditshegon@biust.ac.bw).

The spacer technique is a low-cost fabrication method for fabricating nanowires [7]. It was first reported in 2005 by Ge *et al*., [8] and other researchers [9]-[11] have since carried it forward. The technique has great potential in shaping nanometer features using conventional, low-cost photolithography. The spacer technique uses anisotropic etch to create a vertical pillar on an insulating layer (SiO_2), then after deposition of a semiconductor layer (ZnO) and a second anisotropic etch to create nanowires made up of the semiconductor layer. The method allows nanowire features with controllable dimensions to be developed. The ICP tool is usually used for anisotropic etching and produces surface roughness less than < 1.5 nm. Other tools such as RIE and ion beam etch produce roughness greater than > 5 nm method.

II. Experiment

The experimental procedure for making the NWFET was described in [12]. The device uses Al2O3 as a sensing layer. As listed in Table 1, the dielectric layer is expected to perform better than other commonly used layers. SiO2 contains a lower pH range and sensitivity. The other dielectric layers demonstrate better performance than SiO_2. To make the sensor, SU8-3005 resist was patterned on top of the device to form a sensing well for the bioanalytes, as shown in Fig. 1 [13], [14]. The analyte solutions were different pH solutions with values of 3, 5, 7, and 9.

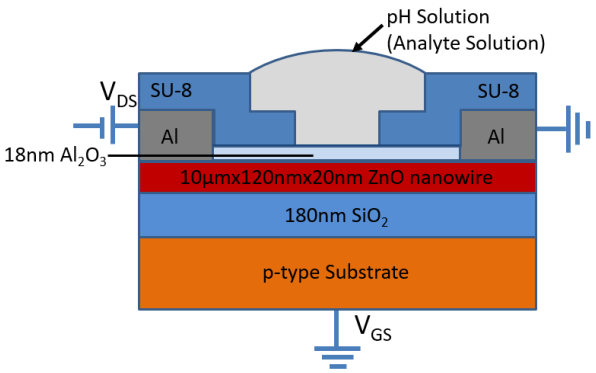

Fig. 1. Arrangement for pH sensing in the fabricated sensor. It shows how analyte solution makes contact with transducer. The sensor contains a channel with 1.7×10^{18} cm^{-3} donor concentration and 100 ZnO nanowires in parallel, each with the following dimensions: 10 µm × 120 nm × 20 nm. The thickness of the underlying SiO_2 is 180 nm. The active channel is passivated with an 18 nm Al_2O_3 layer. Substrate is silicon.

doi: 10.18178/ijeetc.11.2.162-166

TABLE 1: COMPARISON OF THE PH RANGE AND SENSITIVITY OF DIFFERENT SENSITIVE LAYERS ADOPTED FROM [1], [13], [14], [15], [16].

Sensitive layer	pH range	Sensitivity (mV/pH)
SiO_2	2–5	25–48
Al_2O_3	2–12	53–57
Si_3N_4	2–12	46–56
Ta_2O_5	2–12	56–57
HfO_2	2–12	~59

The pH measurements used pH solutions developed by Zeimpekis *et al*. [17], which were created using universal buffer solutions (0.1 M NaCl, 0.01 M citric acid, 0.01 M phosphoric acid, and 0.02 M boric acid adjusted to pH values ranging from 3 to 9 by titration with a 1 M NaOH solution). The fabricated NWFET was observed under SEM [18]-[20] to have a channel length of 20 µm, height of 120 nm, and width of 20 nm. Electrical I-V characterization [21], [22] was performed using the Agilent B1500A semiconductor parametric analyser (Agilent Technologies).

The device was first measured in air, then in liquid, and then in air again. For the liquid measurement, a 5 µL droplet of aqueous solution was introduced in the well to make contact with the channel. After each electrical measurement of a solution with a given pH, the nanowire surface was rinsed with de-ionized water and dried with adsorbent paper. This step was repeated 10 times to remove the pH solution completely. The sequence for measuring the sensor is listed below:

Step 1: The device is measured in air: I_{DS} vs. V_{DS} and I_{DS} vs. V_{GS} (AIR1). The gate sweep rate was set properly for air and pH. V_{DS} and V_{GS} sweep range are checked, followed by a 1 h wait time.

Step 2: pH9 was applied, and then I_{DS} vs. Time (pH9) is measured. After a 3 min wait time, pH9 was removed. DI water was used for rinsing 10 times.

Step 3: pH7 was applied, and I_{DS} vs. Time (pH7) was continually measured. After a 3 min wait time, pH7 was removed. DI water was used for rinsing 10 times.

Step 4: pH5 was applied, and I_{DS} vs. Time (pH5) was continually measured. After a 3 min wait time, pH5 was removed. DI water was used for rinsing 10 times.

Step 5: pH3 was applied, and I_{DS} vs. Time (pH3) was continually measured. After a 3 min wait time, pH3 was removed. DI water was used for rinsing 10 times.

Step 6: pH5 was applied, I_{DS} vs. Time (pH5) was continually measured. After a 3 min wait time, pH5 was removed. DI water was used for rinsing 10 times.

Step 7: pH7 was applied, I_{DS} vs. Time (pH7) was continually measured. After a 3 min wait time, pH7 was removed. DI water was used for rinsing 10 times.

Step 8: pH9 was applied, I_{DS} vs. Time (pH9) was continually measured. After a 3 min wait time, pH9 was removed. DI water was used for rinsing 10 times. After H_2O drying (>24 h), I_{DS} vs. V_{DS} and I_{DS} vs. V_{GS} in air (AIR2) are re-measured.

III. RESULTS AND DISCUSSION

A. Measurement of Sensor in Air-before

The experiment was initially measured with a four-point probe hall measurement tool, which exhibited a sheet resistance of 3.0×10^4 Ω/sq, hall mobility of 5.84 cm²/V-s, and donor concentration of 1.7×10^{18} cm^{-3}. Fig. 2 (a) shows the I_{DS} vs. V_{DS} characteristics of the device, with measurements made in air and darkness at gate biasing from 0 V to 40 V, with steps of 2.0 V, and a drain bias varying from 0 V to 40 V. This produces the maximum currents of 1.5×10^{-4} A at a drain voltage of 40 V. The device shows well-behaved characteristics with good pinch-off and saturation. Fig. 2 (b) shows the I_{DS} vs. V_{GS} characteristics with V_{DS} at 1.0 V. The device possesses a subthreshold slope of 3.0 V/decade, an off current of 1.0×10^{-12} A, a threshold voltage of 11.0 V, and an on/off current ratio of 1.0×10^7.

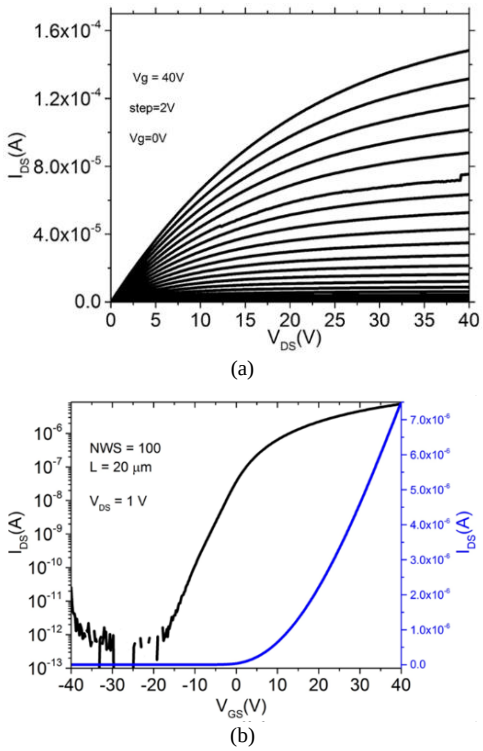

Fig. 2. Sensor electrical characteristics measured in air and darkness: (a) I_{DS} vs. V_{DS} characteristic with a V_{GS} drive from 0 V to 40 V with steps of 2 V and (b) I_{DS} vs. V_{GS} characteristics with V_{DS} = 1.0 V. The NWFET has 100 parallel nanowires and a channel length of L = 20 µm.

B. pH Measurements

Table 2 lists different pH sensors developed at various institutions/laboratories/groups. Sergei V. Dzyadevych *et al*. [23] described the fabrication techniques used for the devices. As previously stated, SiO_2 contains lower pH ranges and sensitivities. However, when it is combined with other dielectrics to create heterojunction structures, the performance is improved. HFO_2 demonstrates the best traits. This makes sense as HFO_2 has a dielectric constant of around 16 which is the highest of all the oxides mentioned in this paper. Fabricated sensors have a sensitivity between approximately 2%/pH (SiO_2 surface) and 4.5%/pH (HfO_2 surface). The designed Al_2O_3 sensor should deliver a sensitivity within this range (2.5%/pH). To improve the sensitivity, the subthreshold slope should be improved by reducing the doping concentration. Equation (1) describes how to derive the sensitivity. The percentage sensitivity can be derived afterwards.

TABLE 2: PROPERTIES OF ISFET PH-SENSORS WITH DIFFERENT GATE MATERIALS [1], [15], [16], [23].

Gate	Sensitivity (mV/pH)	Response and stability	Gate
SiO_2	20–40	non-linear response	SiO_2
SiO2 (40~110 nm, thermally grown) + Si_3N_4 (~100 nm, CVD) on silicon. Channel: 20 µm × 100 µm. Reference electrode: Ag|AgCl|NaCl	~53	Slow response. Sensitivity decreases with time (Formation of oxynitride)	SiO_2 (40~110 nm, thermally grown) + Si_3N_4 (~100 nm, CVD) on silicon. Channel: 20 µm × 100 µm. Reference electrode: Ag|AgCl|NaCl
Al_2O_3	53–57	linear response, very low drift	Al_2O_3
Ta_2O_5	55–59	linear response, undesired light sensitivity	Ta_2O_5

$$\text{Sensitivity}(S)=\frac{\Delta G}{G_0}=\frac{2\varepsilon_r\varepsilon_0\phi_B N(t)}{qa^2 N_D \log\left(1+\frac{t_D}{a}\right)} \quad (1)$$

where ΔG is the change in conductivity of the device, G_0 is the initial conductivity, ε_r is the effective dielectric constant of Al_2O_3, ε_0 is permittivity in vacuum, ϕ_B is the surface potential, $N(t)$ is the density of charge states at the surface, q is the elemental charge, a is a geometry parameter, N_D is the donor concentration, and t_D is the thickness of the dielectric.

Fig. 3 shows the pH results obtained using a liquid gate, with a reference Ag/AgCl electrode that was biased at 50 mV with a drain bias of 100 mV. The substrate was maintained at 0 V bias for all electrical measurements. The low bias on the liquid gate was used to avoid electrolysis in the buffer solution and to minimize any leakage currents while maintaining device operation in the subthreshold region. A field effect transistor acting as a transducer has an advantage over others owing to its high impedance. The high impedance allows for high sensitivity with minimal influence on the target specimen. The device had a total impedance of $2.5\times10^4\ \Omega$ and channel doping of $1.7\times10^{18}\ cm^{-3}$.

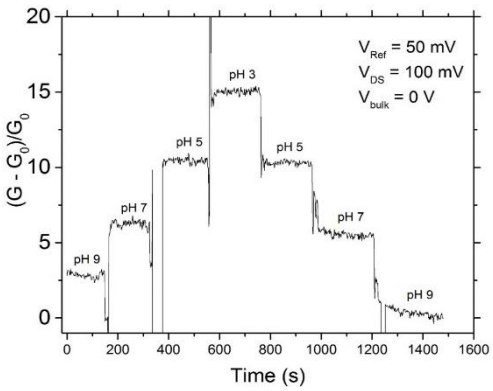

Fig. 3. Graph of normalised sensor conductance change as a function of time. The device measures four different pH values: 9, 7, 5, and 3. The device has a liquid gate with a reference bias of 50 mV, a drain bias of 100 mV, and a substrate bias of 0 V.

This study achieved a pH range of 3–9 and a sensitivity of 2.48 mV/pH to 10.3 mV/pH. The voltage sensitivity translates to a percentage value of 15%. The device shows little to no drift at each pH measurement, which helps to clearly show the current change for the different pH solutions. An abnormally was present when measuring pH 9 again. The device performed poorly.

C. Measurement of Sensor in Air-after

To complete the measurements, the sensor was measured again in air. Fig. 4 shows good transistor characteristics with clear linear, pinch-off, and saturation regions. Fig. 4 (a) shows negative slope of the I_{DS} vs. V_{DS} characteristics due to high gate voltage of around 40V. Fig. 4 (b) exhibits a little strange behavior in the neighborhood of V_{GS}=10V which was due to the introduction of ionic charge at the gate. For values of V_{GS} > 15V the I_{DS} vs. V_{GS} characteristics strongly saturates which must be due to a high serial resistance. The device possesses a subthreshold slope of 1.1 V/decade, an off current of 1.0×10^{-13} A, a threshold voltage of 17 V, and an on/off current ratio of 1.0×10^8. The characteristics were measured at a V_{DS} of 1.0 V.

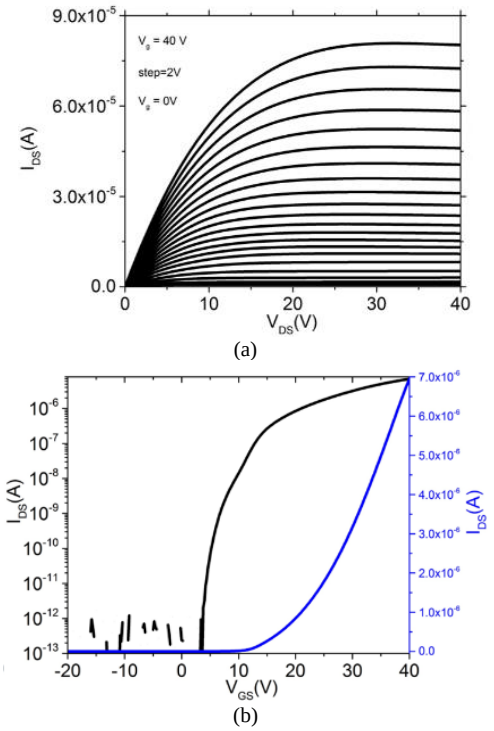

Fig. 4. (a) I_{DS} vs. V_{DS} characteristics of the biosensor devices after pH measurements with a V_{GS} derive from 0 V to 40 V. (b) I_{DS} vs. V_{GS} characteristics of the biosensor devices after pH measurements. The ZnO NWFET biosensor has 100 parallel nanowires and a channel length of L = 20 µm.

D. Comparing I_{DS} vs. V_{DS} Measurements before and after pH Measurements

Fig. 5 (a) shows subthreshold I_{DS} vs. V_{DS} graphs before and after the pH measurements. Before pH sensing, the curve has a subthreshold slope of 3.0 V/decade, a threshold voltage of 11.0 V, an off current of 1.0×10^{-12} A, and an on/off current ratio of 1.0×10^7. After pH sensing, the curve has a subthreshold slope of 1.1 V/decade, a

threshold voltage of 23 V, an off current of 1.0×10^{-13} A, and on/off current ratio of 1.0×10^{8}. These values were derived at V_{DS} = 1.0 V. Fig. 5 (b) shows a comparison of the linear I_{DS} vs. V_{DS} characteristics before and after the pH measurements. The sensor retained good transistor characteristics with no evidence that the liquid environment significantly degraded the transistor characteristics. However, there are some significant changes in the characteristics. Thus, there may have been some liquid penetration through the passivating Al_2O_3 layer and ZnO layer to the gate oxide interface.

Fig. 6 shows the transconductance verses V_{GS} plot for the device measured before and after the pH measurements. The curve for the device before the pH measurements has a peak transconductance of 3.0×10^{-7} S at 40.0 V, whereas the curve for the device after the pH measurements has peak transconductance of 4.0×10^{-7} S at 37.0 V. Using peak values of transconductance, the field effect mobility (μ_{FE}) is derived for both measurements. The curve before has a μ_{FE} of 32.5 cm^2/Vs, whereas the curve after has a μ_{FE} of 42.9 cm^2/Vs.

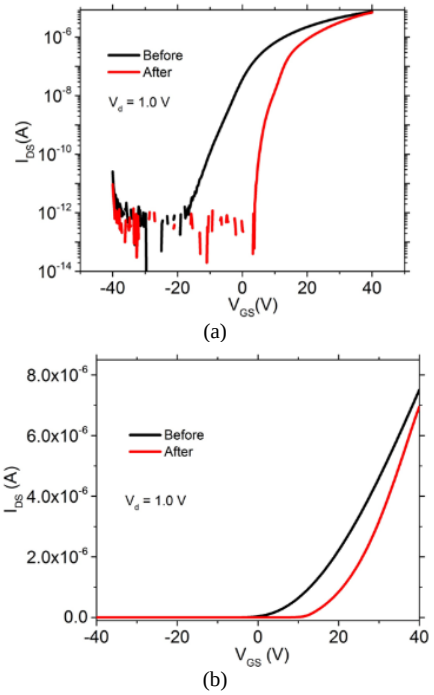

Fig. 5. (a) Subthreshold I_{DS} vs. V_{GS} characteristics before and after the pH measurements. These values were derived at V_{DS} = 1.0 V. Image (b) shows the linear I_{DS} vs. V_{GS} characteristics before and after the pH measurements.

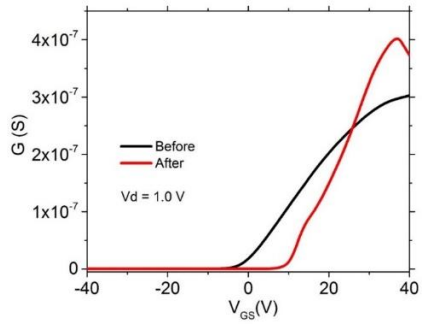

Fig. 6. Transconductance verses gate voltage for the sensor before and after the pH measurements.

IV. Conclusion

A ZnO NWFET pH sensor was fabricated and measured. The device was measured under a controlled environment with and without pH solutions. The results are comparable to those of manufactured ISFETs. The pH range was 3–9 with a sensitivity of 2.48 mV/pH to 10.3 mV/pH. The voltage sensitivity translates to a percentage value of 15%. The device was measured before and after the pH solution treatment, demonstrating that through rinsing and brushing the sensing layer, the device can be re-used.

Conflict of Interest

The authors declare no conflict of interest.

Acknowledgment

The author would like to acknowledge the Botswana International University of Science and Technology (BIUST) for supporting his doctoral studies and the Southampton Nanofabrication Centre for the experimental work. The author would also like to acknowledge EPSRC EP/K502327/1 for grant support.

References

[1] J. C. Dutta, "Ion sensitive field effect transistor for applications in bioelectronic sensors: A research review," in *Proc. of CISP2012*, 2012, pp. 185–191.

[2] N. M. J. Ditshego, "ZnO nanowire field effect transistor for biosensing: A review," *Journal of Nano Research*, vol. 60, pp. 94-112, 2019.

[3] A. Wei, L. Pan, and W. Huang, "Recent progress in the ZnO nanostructure-based sensors," *Mater. Sci. Eng. B*, vol. 176, no. 18, pp. 1409–1421, Nov. 2011.

[4] B. R. Huang, J. C. Lin, and Y. K. Yang, "ZnO/silicon nanowire hybrids extended-gate field-effect transistors as pH sensors," *J. Electrochem. Soc*., vol. 160, no. 6, pp. B78–B82, Apr. 2013.

[5] P. Y. Yang, J. L. Wang, P. C. Chiu, J. C. Chou, C. W. Chen, H. H. Li, and H. C. Cheng, "pH sensing characteristics of extended-gate field-effect transistor based on Al-doped ZnO nanostructures hydrothermally synthesized at low temperatures," *IEEE Electron Device Lett.*, vol. 32, no. 11, pp. 1603–1605, Nov. 2011.

[6] S. P. Chang, C. W. Li, K. J. Chen, S. J. Chang, C. L. Hsu, T. J. Hsueh, and H. T. Hsueh, "ZnO-nanowire-based extended-gate field-effect-transistor pH sensors prepared on glass substrate," *Sci. Adv. Mater*., vol. 4, no. 11, pp. 1174–1178, Nov. 2012.

[7] N. M. J. Ditshego, N. A. B. Ghazali, M. Ebert, K. Sun, I. Zeimpekis, P. Ashburn, M. R. R. De Planque, and H. M. H. Chong, "ZnO nanowire-FET for charge-based sensing of protein biomolecules", in *Proc. IEEE 15th Int. Conf. on Nanotechnology*, 2015, pp. 801-804.

[8] H. Ge, W. Wu, Z. Li, G.-Y. Jung, D. Olynick, Y. Chen, J. A. Liddle, S. Y. Wang, and R. S. Williams, "Cross-linked polymer replica of a nanoimprint mold at 30 nm half-pitch.," *Nano Lett.*, vol. 5, no. 1, pp. 179–82, Jan. 2005.

[9] H. W. Ra, K. S. Choi, J. H. Kim, Y. B. Hahn, and Y. H. Im, "Fabrication of ZnO nanowires using nanoscale spacer lithography for gas sensors," *Small*, vol. 4, no. 8, pp. 1105–9, Aug. 2008.

[10] T. Weber, T. Käsebier, A. Szeghalmi, M. Knez, E. B. Kley, and A. Tünnermann, "Iridium wire grid polarizer fabricated using atomic layer deposition," *Nanoscale Research Letters*, vol. 6, Oct. 2011.

[11] X. Liu, X. Deng, P. Sciortino, M. Buonanno, F. Walters, R. Varghese, J. Bacon, L. Chen, N. O'Brien, and J. J. Wang, "Large area, 38 nm half-pitch grating fabrication by using atomic spacer

lithography from aluminum wire grids.," *Nano Lett.*, vol. 6, no. 12, pp. 2723–7, Dec. 2006.

[12] N. M. J. Ditshego and S. M. Sultan, "Top-down fabrication process of ZnO NWFETs," *J. Nano Res.*, vol. 57, pp. 77–92, Apr. 2019.

[13] T. E. Bae, H. J. Jang, J. H. Yang, and W. J. Cho, "High performance of silicon nanowire-based biosensors using a high-K stacked sensing thin film," *ACS Appl. Mater. Inter.*, vol. 5, no. 11, pp. 5214–5218, May 2013.

[14] B. Reddy, B. R. Dorvel, J. Go, P. R. Nair, O. H. Elibol, G. M. Credo, J. S. Daniels, E. K. C. Chow, X. Su, M. Varma, M. A. Alam, and R. Bashir, "High-k dielectric Al_2O_3 nanowire and nanoplate field effect sensors for improved pH sensing," *Biomed. Microdevices*, vol. 13, no. 2, pp. 335–44, Apr. 2011.

[15] S. A. Pullano, N. T. Tasneem, I. Mahbub, S. Shamsir, M. Greco, S. K. Islam, and A. S. Fiorillo, "Deep submicron EGFET based on transistor association technique for chemical sensing," *Sensors*, vol. 19, pp. 1063-1076, March 2019.

[16] P. Kurzweil, "Metal oxides and ion-exchanging surfaces as pH sensors in liquids: State-of-the-art and outlook," *Sensors*, vol. 9, pp. 4955-4985, 2009.

[17] I. Zeimpekis, K. Sun, C. Hu, N. M. J. Ditshego, O. Thomas, M. R. R. D. Planque, H. M. H. Chong, H. Morgan, and P. Ashburn, "Dual-gate polysilicon nanoribbon biosensors enable high sensitivity detection of proteins," *Nanotechnology*, vol. 27, no. 16, pp. 165502-165509, 2016.

[18] S. Ghosh and L. Rajan, "Zinc oxide thin-film transistor with catalytic electrodes for hydrogen sensing at room temperature," *IEEE Trans. on Nanotechnology*, vol. 20, pp. 303-310, Mar. 2021.

[19] K. Lu, R. Yao, Wei Xu, H. Ning, X. Zhang, G. Zhang, Y. Li, J. Zhong, Y. Yang, and J. Peng, "Alloy-electrode-assisted high-performance enhancement-type neodymium-doped indium-zinc-oxide thin-film transistors on polyimide flexible substrate," *Research*, vol. 2021, 2021.

[20] R. C. Hoffmann, S. Sanctis, M. O. Liedke, M. Butterling, A. Wagner, C. Njel, and J. J. Schneider, "Zinc oxide defect microstructure and surface chemistry derived from oxidation of metallic zinc: Thin-film transistor and sensor behavior of ZnO films and rods," *Chemistry—A European Journal*, vol. 27, no. 17, pp. 5422-5431, 2021.

[21] B. Bekele, A. Degefa, F. Tesgera, L. T. Jule, R. Shanmugam, L. P. Dwarampudi, N. Nagaprasad, and K. Ramasamy, "Green versus chemical precipitation methods of preparing zinc oxide nanoparticles and investigation of antimicrobial properties," *Journal of Nanomaterials*, vol. 2021, Sept. 2021.

[22] W. M. Abdelraheem and E. S. Mohamed, "The effect of zinc oxide nanoparticles on pseudomonas aeruginosa biofilm formation and virulence genes expression," *J. Infect Dev Ctries*, vol. 15, no. 06, pp. 826-832, Jun. 2021.

[23] S. V. Dzyadevych, A. P. Soldatkin, A. V. El'skaya, C. Martelet, and N. Jaffrezic-Renault, "Enzyme biosensors based on ion-selective field effect transistors," *Analytica Chimica Acta*, vol. 568, pp. 248–258, May 2006

Nonofo M. J. Ditshego is a senior lecturer at Botswana International University of Science and Technology (BIUST) in the School of Electrical, Computer and Telecommunications Engineering. He received his MEng and PhD from University of Southampton, UK. After receiving his MEng degree. In 2012, he enrolled for PhD studies in Electronic and Electrical Engineering under the supervision of Prof. P. Ashburn, Dr M. R. R. de Plaque and Dr. H. M. H Chong. The PhD project was based on 3D modelling, simulation and fabrication of zinc oxide nanowire field effect transistor for biosensing. The device is an emerging non-planar technology and is still at an embryonic stage from an industrial point of view.